誌説 EDITORIAL

Save the meniscus

半月板は血行が辺縁側の30%に限られ，細胞の密度が低く，荷重によるストレスにさらされるため，損傷すると自然治癒しにくい．日本では，半月板損傷に対する唯一の温存手術は半月板縫合術である．代表的な教科書には，「若年者の辺縁部縦断裂には縫合を行う．水平断裂や横断裂には部分切除を行う．中高年の断裂半月は変性をきたしており，部分切除されることが多い」と記載されており，縫合術の一般的な手術適応は限定されている．断裂形式以外にも，スポーツや職場への復帰を早期に確実に目指そうとする意識や，外科医としてまれでない半月板縫合後の再断裂を避けたいという意識が働き，半月板切除術が選択されることが多いと思われる．平成24年度厚生労働省社会医療診療行為別調査によると，日本の半月板手術は年間に約3万件で，そのうち縫合術はわずか8%のみであり，90%以上が切除術であった．

半月板を広範囲に切除すると，衝撃緩衝・荷重分散・安定性保持等の半月板が有する機能が消失し，隣接する関節軟骨の摩耗や変性が進行し，変形性膝関節症が必発する．また，部分切除でさえも，半月板の主要な円周状線維の連続性が途絶し，フープストレスに抗しきれなくなり，半月板は逸脱し，半月板機能が破綻し，変形性膝関節症を進行させる．世界でも比類なき超高齢社会を迎えている我が国において，変形性膝関節症は運動器疾患の解決するべき大問題であり，できる限り変形性膝関節症の発症を抑えることに努めなければならない．

ここで二つの臨床研究を紹介したい．Englundらは50歳以上の一般住民991名に対して，MRI検査と膝症状の問診を行った．膝の症状がないにもかかわらず，MRIで半月板の異常像を呈した割合は61%であった[1]．Katzらは45歳以上の軽中等度変形性膝関節症を呈した症候性の半月板損傷患者351名を部分切除群と運動療法群に分けて比較した．疼痛や膝機能は6ヵ月後に2群間で変わらなかった[2]．この2編の論文は，MRIで検出される半月板異常像は必ずしも疼痛の原因にはならず，半月板切除術の適応は慎重に考えるべきであることを示している．

私たちはこれまで軟骨損傷や変形性膝関節症の病変部位に対して，滑膜由来の未分化な体性幹細胞を関節鏡視下に移植する再生医療を行ってきた．大腿骨顆部に対しては概ね良好な成績が得られている．しかし，半月板がすでに切除されている症例では軟骨再生が十分でない例があり，また活動量を下げている間は関節軟骨が再生されても運動レベルを上げると数年後に再び摩耗する例もある．未分化な幹細胞を微小環境に応じて分化させるためには，周囲からの適切なメカニカルストレスが必要であり，大腿骨顆部の軟骨病変を未分化な幹細胞を使用して再生させるためには，半月板から幹細胞へのメカニカルストレスが重要であることが予測される．また，一度関節軟骨が再生されても，半月板がなければ活動量を上げると関節軟骨の摩耗が急激に進むことは，正常軟骨の場合と同様である．

半月板を縫合するための器具の開発や技術の進歩により，半月板縫合術の成績はこれまでのものよりもよくなることが期待される．また，変性した半月板でも切除するよりは残存させるほうが，関節軟骨の保護にとっては望ましいであろう．今後，医療技術が発達して半月板機能を再獲得できる再生医療が可能となる時代がくるかもしれないが，完全に切除された半月板をゼロから再生させるよりも，たとえ変性していても残っている半月板を利用するほうがより容易であると感じる．またすべての変形性膝関節症を再生させることは困難であるが，骨切り術や半月板の制動術等と組み合わせることにより，あるカテゴリーの変形性膝関節症は再生できる可能性がある．しかしこれは，変性していても半月板機能が残存していることが前提となるであろう．

Save the meniscus as much as possible!

文　献

1) Englund M, Guermazi A, Gale D et al：Incidental meniscal findings on knee MRI in middle-aged and elderly persons. N Engl J Med **359**：1108-1115, 2008
2) Katz JN, Brophy RH, Chaisson CE et al：Surgery versus physical therapy for a meniscal tear and osteoarthritis. N Engl J Med **368**：1675-1684, 2013

（東京医科歯科大学再生医療研究センター教授・
関矢一郎）

Use of a Comprehensive Polymerase Chain Reaction System for Diagnosis of Ocular Infectious Diseases

Sunao Sugita, MD, PhD,[1,2] Manabu Ogawa, MD, PhD,[1] Norio Shimizu, PhD,[3] Tomohiro Morio, MD, PhD,[4] Nobuyuki Ohguro, MD, PhD,[5] Kei Nakai, MD, PhD,[6] Kazuichi Maruyama, MD, PhD,[7] Kenji Nagata, MD,[7] Atsunobu Takeda, MD, PhD,[8] Yoshihiko Usui, MD, PhD,[9] Koh-Hei Sonoda, MD, PhD,[10] Masaru Takeuchi, MD, PhD,[11] Manabu Mochizuki, MD, PhD[1]

Purpose: To measure the genomic DNA of ocular infectious pathogens in ocular fluids and to analyze the clinical relevance of these pathogens in uveitis and endophthalmitis.

Design: Prospective clinical case series.

Participants: A total of 500 patients with infectious uveitis and endophthalmitis were examined at Tokyo Medical and Dental University, Tokyo Medical University, Kyushu University, Osaka University, and Kyoto Prefectural University, all in Japan.

Methods: Genomic DNA of bacteria, fungi, parasites, and viruses in collected intraocular samples were examined by comprehensive polymerase chain reaction (PCR). Samples were analyzed first by multiplex PCR and quantitative real-time PCR for human herpes viruses (HHVs) 1 through 8 and toxoplasma. Subsequently, samples were examined by broad-range real-time PCR for bacterial 16S and fungal 18S/28S ribosomal DNA (rDNA).

Main Outcome Measures: Infectious uveitis and endophthalmitis diagnoses were obtained when using the PCR system. Calculations of the positivity and the diagnostic parameters such as sensitivity, specificity, positive predictive value (PPV), and negative predictive value (NPV) also were evaluated.

Results: In all of the tested infectious uveitis and endophthalmitis patients, either herpes simplex virus type 1 (n = 18), herpes simplex virus type 2 (n = 4), varicella-zoster virus (n = 55), Epstein-Barr virus (n = 17), cytomegalovirus (n = 68), HHV type 6 (n = 2), toxoplasma (n = 6), bacterial 16S (n = 33), or fungal 18S/28S (n = 11) genome was detected. Neither HHV type 7 nor HHV type 8 DNA was detected in any of the samples. Of the 21 false-negative results found during the PCR analyses, 12 cases were negative for patients clinically suspected of having bacterial endophthalmitis. Conversely, false-positive results for the comprehensive PCR examinations occurred in only 3 cases that subsequently were found to have bacterial 16S rDNA. Diagnostic parameters for the sensitivity, specificity, PPV, and NPV of our PCR examinations were 91.3%, 98.8%, 98.6%, and 92.4%, respectively.

Conclusions: Use of our comprehensive PCR assay to examine ocular samples in patients with endophthalmitis and uveitis seems to be clinically useful for detecting infectious antigen DNA. Thus, this PCR method is a reliable tool for both diagnosing ocular disorders and further screening of patients for intraocular infections.

Financial Disclosure(s): The author(s) have no proprietary or commercial interest in any materials discussed in this article. *Ophthalmology 2013;120:1761–1768 © 2013 by the American Academy of Ophthalmology.*

Infectious uveitis and endophthalmitis are sight-threatening diseases caused by human pathogenic agents. Virus infections, especially herpes viruses, are known to cause ocular inflammations such as retinitis, uveitis, retinal vasculitis, conjunctivitis, corneal endotheliitis, and keratitis. Parasitic infections (e.g., ocular toxoplasmosis) are known to cause intraocular inflammations such as uveitis, whereas bacterial and fungal infections are known to cause endophthalmitis, uveitis, and keratitis. However, when infectious pathogens cause ocular inflammatory disorders, the clinical findings can be very diverse, thereby making the diagnosis of the infection both difficult and time consuming. To ensure that appropriate treatments are performed that will prevent these infectious agents from causing irreversible ocular tissue damage, early examinations that correctly identify the cause of the infections are a necessity.

For more than a decade, diagnostic evaluations of patients with uveitis and endophthalmitis diagnoses have included the use of conventional qualitative polymerase chain reaction (PCR). A PCR diagnosis has proven to be very useful because only a very small sample is required for detection of the infectious agents. However, in the past, the relatively small volume of sample that can be obtained (such as aqueous humor) has made it impossible to conduct comprehensive examinations for ocular inflammatory diseases. Nevertheless, comprehensive diagnoses are needed

ISSN 0161-6420/13/$–see front matter
http://dx.doi.org/10.1016/j.ophtha.2013.02.020

because ocular inflammatory diseases can include various infectious antigens. Additionally, because sudden changes can occur in ocular infectious diseases, it is imperative that patients be diagnosed as early as possible. Therefore, a comprehensive, rapid, and accurate diagnosis using ocular samples is of great importance, and if such a comprehensive PCR system for the diagnosis of ocular infectious disorders could be established, this would be a tremendous help for many clinicians. However, this research tool has not been widely available for use in clinical laboratories. Therefore, this study attempted both to establish novel tests that would be widely available to clinical laboratories and to develop a comprehensive PCR system that could be used to examine bacteria, fungi, parasites, and viruses for the purpose of diagnosing ocular infectious disorders.

Methods

Patients

Intraocular samples of aqueous humor and vitreous fluid were collected from 500 patients with uveitis and endophthalmitis. Underlying pathologic features included endotheliitis, keratouveitis, anterior uveitis or iridocyclitis, acute retinal necrosis (ARN), progressive outer retinal necrosis, cytomegalovirus (CMV) retinitis, human T lymphotropic virus type 1 uveitis, ocular toxoplasmosis, scleritis, Posner-Schlossman syndrome, Fuchs' iridocyclitis, sarcoidosis, Vogt-Koyanagi-Harada disease, Behçet's disease, intraocular lymphoma, idiopathic uveitis, idiopathic retinal vasculitis, bacterial endophthalmitis, and fungal endophthalmitis. At the time of sampling, these patients displayed active intraocular inflammation. In addition, control samples were prepared for this study (n = 100). The control group included noninflammatory diseases such as diabetes, retinal detachment, glaucoma, and others.

An aliquot of 0.1 ml aqueous humor was aspirated with a 30-gauge needle. Nondiluted vitreous fluid samples were collected from uveitis patients who were undergoing vitreous surgery (diagnostic pars plana vitrectomy). Samples were transferred into presterilized microfuge tubes and used for PCR. To ensure that no contamination of the PCR preparation occurred, the DNA amplification and the analysis of the amplified products were carried out in separate laboratories according to a method reported in a previous study.[1]

We consecutively enrolled endophthalmitis and uveitis patients from 2006 through 2010 for a prospective study that was conducted at both our hospital facility (Tokyo Medical and Dental University) and its associated hospitals (Tokyo Medical University, Kyushu University, Osaka University, and Kyoto Prefectural University). After informed consent was obtained from all patients, we collected aqueous humor and vitreous fluid samples. The research followed the tenets of the Declaration of Helsinki and all study protocols were approved by the Institutional Ethics Committees of Tokyo Medical and Dental University and its associated hospitals. The clinical trial was registered on September 7, 2009 (available at: www.umin.ac.jp/ctr/index/-j.htm; study no.: R000002708).

Polymerase Chain Reaction Analyses

The sampling procedure and the PCR methodology are shown in Figure 1. DNA was extracted from the samples using a DNA Mini kit (Qiagen, Valencia, CA) installed on a robotic workstation that was set for automated purification of nucleic acids (BioRobot EZ1 Advanced; Qiagen). Genomic DNA of human herpes virus (HHV), toxoplasma, bacteria, and fungi in the aqueous humor and vitreous fluids was measured through the use of 2 independent PCR assays: (1) a qualitative multiplex PCR that was performed in conjunction with a quantitative real-time PCR, and (2) a broad-range real-time PCR (Fig 1). The multiplex PCR qualitatively measured the genomic DNA of 8 HHVs: herpes simplex virus (HSV) type 1 (HHV-1), HSV-2 (HHV-2), varicella-zoster virus (VZV; HHV-3), Epstein-Barr virus (EBV; HHV-4), CMV (HHV-5), HHV-6, HHV-7, HHV-8, and toxoplasma. The PCR was performed using a LightCycler 480 II instrument (Roche, Basel, Switzerland). If the multiplex PCR results were positive, we then conducted real-time PCR. The real-time PCR was performed using the Amplitaq Gold and the Real-Time PCR 7300 system (Applied Biosystems, Foster City, CA) or the LightCycler 480 II instrument (Roche). Primers and probes for HHV types 1 through 8 and the PCR conditions have been described previously.[2,3] The toxoplasmosis primers and probes also have been reported previously.[4]

To detect DNA for bacterial species (Fig 1), broad-range PCR was performed using the Amplitaq Gold and the Real-Time PCR 7300 system or the LightCycler 480 II instrument in accordance with our previously reported methodology.[1] Primers and probes for the fungal species (fungal 18S or 28S ribosomal DNA [rDNA]) along with the PCR conditions also have been reported previously.[5,6]

Amplification of the human β-globulin gene served as an internal positive extraction and amplification control. The value of the HHV copy number in the sample was considered to be significant when more than 50 copies/ml were observed. Significant differences in the copy number were defined as more than 10 copies/ml for toxoplasmosis, more than 100 copies/ml for bacterial 16S, and more than 10 copies/ml for fungal 18S/28S.

Results

Step 1 of our comprehensive PCR examinations consisted of qualitative multiplex PCR combined with quantitative real-time PCR, whereas step 2 used broad-range real-time PCR (Figs 1 and 2). As seen in the results for a representative positive aqueous humor sample, although we observed a high copy number of bacterial 16S rDNA, the PCR examination indicated that the sample showed negative results for DNA from all other infectious antigens (Fig 2).

In the uveitis and endophthalmitis patients, our comprehensive PCR system results demonstrated positivity in the ocular fluids. As seen in Table 1, multiplex PCR and real-time PCR detected 18 patients with HSV-1 DNA (18 of 500 cases; 3.6% positive). Herpes simplex virus type 2 DNA was detected in only 4 patients (0.8% positive), with all of these patients subsequently diagnosed with ARN. Varicella-zoster virus DNA was detected in the ocular fluid samples of 55 patients (11% positive), whereas EBV DNA was detected in 17 patients (3.4% positive) with various ocular inflammatory disorders. Cytomegalovirus was detected in 68 patients (13.6% positive) with disorders that included corneal endotheliitis, iridocyclitis, and necrotic retinitis. However, our PCR methods detected only 2 HHV-6 DNA cases (0.4% positive), with none of the patients found to have HHV-7 or HHV-8. In addition, toxoplasmosis DNA was detected in only 6 samples (1.2% positive), with all of these patients found to have active uveitis with ocular toxoplasmosis. Overall, our multiplex PCR and real-time PCR analyses identified 170 PCR-positive patients (34% positive; Table 1).

However, when we used broad-range real-time PCR to screen for detection of bacterial 16S and fungal 18S/28S rDNA in infec-

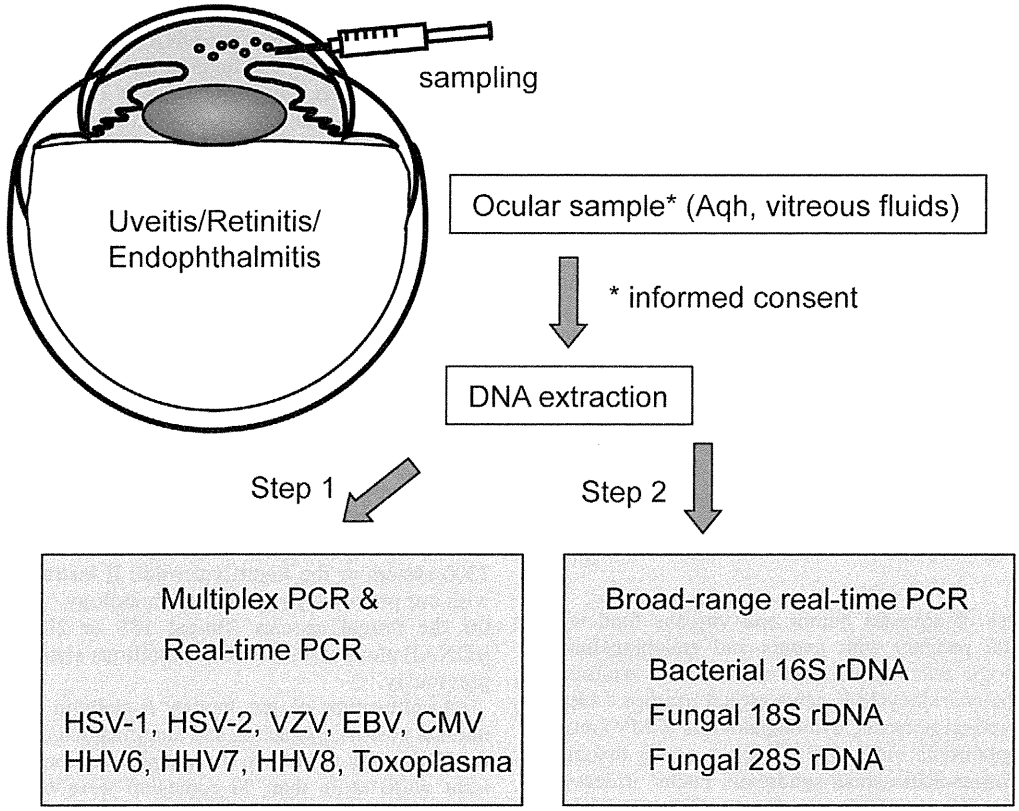

Figure 1. Diagram showing the use of a comprehensive polymerase chain reaction (PCR) system for the analysis of various infectious genomic DNA in the ocular fluids of patients with uveitis and endophthalmitis. To detect various infectious agents, we used independent PCR methods, with step 1 using multiplex PCR and real-time PCR and step 2 using broad-range real-time PCR. After DNA extraction from each of the samples, multiplex PCR was performed first to screen for human herpes virus type 1 (HHV1) to human herpes virus type 8 (HHV8) and for toxoplasmosis via the use of 3 LightCycler capillaries (Roche, Basel, Switzerland). If positive results was observed, real-time PCR was performed subsequently to measure the DNA load. Step 2 used broad-range real-time PCR for detection of bacterial 16S, fungal 18S, or fungal 28S ribosomal DNA (rDNA). To be able to detect the various bacterial and fungal DNAs, primers and probes for the unvariable regions in the sequences were used. Aqh = aqueous humor; CMV = cytomegalovirus; EBV = Epstein-Barr virus; HHV6 = human herpes virus type 6; HHV7 = human herpes virus type 7; HSV-1 = herpes simplex virus type 1; HSV-2 = herpes simplex virus type 2; VZV = varicella-zoster virus.

tious endophthalmitis, we detected 33 patients with bacterial 16S rDNA (33 of 500 cases; 6.6% positive; Table 1). In 11 patients, fungal 18S/28S rDNA was detected in the ocular fluid samples (2.2% positive). Overall, broad-range real-time PCR analysis identified 44 PCR-positive endophthalmitis patients (8.8% positive; Table 1). Analysis of the control samples from patients without intraocular inflammation (n = 100) showed that all had negative results.

Subsequently, we analyzed the results for each of the infectious antigens, including HHV-1 through HHV-8, toxoplasma, bacteria, and fungi. Table 2 shows a summary of the results. Herpes simplex virus type 1 was detected in 1 case of keratouveitis, in 16 cases of anterior uveitis, and in 1 case of ARN, whereas HSV-2 was detected in 4 cases of ARN. Varicella-zoster virus was detected in two cases of keratouveitis, 26 cases of anterior uveitis, 24 cases of ARN, and in two cases of progressive outer retinal necrosis. Epstein-Barr virus was detected in 5 cases of idiopathic uveitis. In addition, EBV also was detected in patients with various ocular inflammatory disorders and intraocular lymphoma (Table 2).

Cytomegalovirus was detected in many cases of corneal endotheliitis (11 of 12 patients), iridocyclitis (anterior uveitis; 32 of 76 patients), and CMV-associated necrotic retinitis (23 of 23 patients). Human herpes virus type 6 was detected in 2 cases of bacterial endophthalmitis. Both of these cases exhibited typical bacterial infections of the eye. Human herpes virus type 7 and HHV-8 DNA were not detected in any of the patients in this study (Table 2). Toxoplasma DNA was detected in active uveitis with ocular toxoplasmosis (n = 6), but not in any of the other ocular inflammatory cases.

Broad-range real-time PCR examinations found bacterial 16S rDNA in 26 cases of bacterial endophthalmitis, in 3 cases of idiopathic uveitis, and in 4 cases of other types of infections. Fungal 18S/28S rDNA was detected in 9 cases of fungal endophthalmitis, in 1 case of idiopathic uveitis, and in 1 case with another infection (Table 2).

We also analyzed whether this PCR examination included any false-negative or false-positive results. A false-negative result indicated that although the PCR results were negative, the patient ultimately was diagnosed with an ocular infection by other examinations or clinical findings or by their responses to treatment. Overall, we determined there were 21 false-negative results in this analysis (Table 3). Among these, the PCR results were negative in 12 cases even though the patients were suspected clinically of having bacterial endophthalmitis. However, false-positive results indicated there were positive PCR results, even though patients finally were diagnosed as having a clinically noninfectious disorder. Overall, there were 3 false-positive results for the PCR anal-

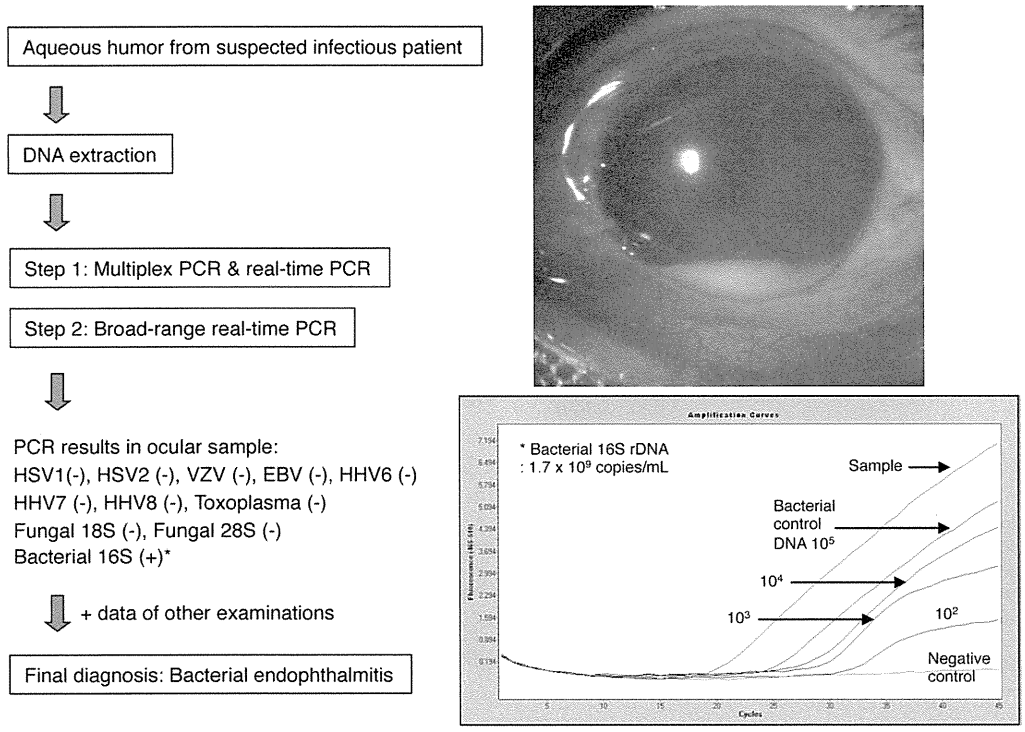

Figure 2. Polymerase chain reaction (PCR) results for a sample from a representative case. An aqueous humor sample was obtained from an endophthalmitis patient (severe anterior chamber cells with hypopyon in the slit photograph on the right). After DNA extraction from the sample, multiplex PCR was performed to screen for human herpes virus types 1 through 8 (HHV1–8) and *Toxoplasmosis gondii* using LightCycler capillaries. We simultaneously performed broad-range real-time PCR for the detection of bacterial 16S or fungal 18S/28S ribosomal DNA (rDNA) and found there was a high copy number of bacterial 16S rDNA in the sample. The sample demonstrated negative results for the human herpes viruses (HSV), such as HSV1, HSV2, varicella-zoster virus (VZV), Epstein-Barr virus (EBV), cytomegalovirus (CMV), HHV6, HHV7, and HHV8 for *T. gondii*. Broad-range real-time PCR indicated the sample showed negative results for fungal 18S and 28S rDNA. The patient finally was diagnosed as having infectious endophthalmitis related to bacterial infections.

ysis, with each case confirmed to contain bacterial 16S rDNA (Table 4).

We also analyzed our comprehensive PCR examinations for the diagnosis of ocular infection in terms of the diagnostic parameters for sensitivity, specificity, positive predictive value, and negative predictive value. The calculated percentages for sensitivity, specificity, positive predictive value, and negative predictive value were 91.3%, 98.8%, 98.6%, and 92.4%, respectively.

Discussion

In the field of ophthalmology, PCR has proven to be very useful for patient diagnosis because the analysis can be carried out using only a very small amount of sample, such as aqueous humor. When comprehensive PCR is used, the results make it possible to include or exclude infections as the potential cause of an ocular disorder. When using our PCR system, a diagnosis can be made quickly, and in fact is much less time consuming compared with other methods. For example, multiplex PCR requires only 90 minutes, real-time PCR takes 60 minutes, and DNA extraction can be performed in only 40 minutes. Additionally, the diagnostic parameters (sensitivity, specificity, positive predictive value, and negative predictive value) of these comprehensive PCR examinations are very high. Even so, it should be noted that with regard to the sensitivity and specificity, there is no agreed upon gold standard, which could lead to difficulties when making a diagnosis. However, from a clinical aspect, use of these comprehensive PCR examinations to analyze ocular samples makes it possible to diagnose rapidly patients with unknown intraocular infectious disorders such as uveitis and endophthalmitis.

With multiplex PCR, it is possible to screen rapidly for the genome of more than 10 types of infectious antigens.[2–4] Additionally, when the PCR screening results are positive, this real-time PCR then can be used to measure the DNA load. Thus, use of this real-time PCR makes it possible to obtain quantitative information for antigen DNA in samples. Recently, broad-range real-time PCR for bacteria or fungi has become available.[1,5,6] With this method, we were able to measure the amplification of the target rDNA genes. Target antigens for this method include the bacteria 16S,[1] fungal 28S,[6] and *Candida* or *Aspergillus* 18S rRNA genes.[5] Detection of bacterial or fungal DNA is possible because primers and probes can be designed specifically for the unvariable regions (bacterial or fungal common regions) within the sequences. By using the primers and probes of these genes, broad-range PCR can be used to detect the presence of bacteria or fungi in the samples.

Table 1. Positivity of the Comprehensive Polymerase Chain Reaction System in the Ocular Fluids of 500 Patients with Uveitis and Endophthalmitis

Infectious Antigens	Multiplex PCR and Real-Time PCR	Broad-Range Real-Time PCR
HSV-1 (HHV-1)	18/500 (3.6%)	—
HSV-2 (HHV-2)	4/500 (0.8%)	—
VZV (HHV-3)	55/500 (11.0%)	—
EBV (HHV-4)	17/500 (3.4%)	—
CMV (HHV-5)	68/500 (13.6%)	—
HHV-6	2/500 (0.4%)	—
HHV-7	0/500 (0%)	—
HHV-8	0/500 (0%)	—
Toxoplasmosis	6/500 (1.2%)	—
Bacteria 16S	—	33/500 (6.6%)
Fungal 18S/28S	—	11/500 (2.2%)
Total	170/500 (34.0%)	44/500 (8.8%)

CMV = cytomegalovirus; EBV = Epstein-Barr virus; HHV-1 through HHV-8 = human herpes virus types 1 through 8; HSV-1 and HSV-2 = herpes simplex virus types 1 and 2; VZV = varicella-zoster virus.
Multiplex polymerase chain reaction (PCR) and real-time PCR were performed to screen for or detect HHV genomic DNA and toxoplasmosis. Broad-range real-time PCR was performed to screen for and detect bacterial 16S and fungal 18S/28S ribosomal DNA.

Based on PCR results, clinical findings, and other examinations, we were able to diagnose infectious diseases successfully. In the present study, with the exception of HHV-7 and HHV-8, almost all of the infectious agents were detected in collected ocular samples. Herpes simplex virus type 1 was detected in aqueous humor of patients with keratouveitis, anterior uveitis, and ARN. However, the symptoms in 4 ARN patients were shown to be related to an HSV-2 infection. In addition to detecting VZV DNA in many ocular samples, our results also indicated a high copy number of VZV DNA in the samples. We previously reported finding an association between the VZV viral load in the aqueous humor and the clinical manifestations of VZV anterior uveitis.[7] Iris atrophy was found to be much more severe in the high-viral load group compared with the low-viral load group. Overall, our results demonstrated that there was a significant correlation between the VZV viral load in the aqueous humor and damage to the iris, such as iris atrophy and pupil distortion, in patients with VZV-related anterior uveitis.

Multiplex and real-time PCR analysis of samples from various infectious patients detected EBV DNA in 17 of 500 cases (3.4%). In a previous study,[8] we found only 3 of 17 samples from uveitis patients to have significantly high EBV DNA copy numbers when using real-time PCR. Because the EBV viral load was not very high in these samples, this suggested that viral replication of EBV does not occur in the eye. It has been assumed that the EBV infection acts as a secondary factor in the pathogenesis of ocular inflammation.[9] Epstein-Barr virus has been shown to be able to infect B-lymphocytes and epithelial cells, including ocular pigment epithelial cells.[10] Therefore, it may be the intraocular infiltrating B-cells and the epithelial cells that are releasing the EBV DNA within the eye during inflammatory conditions. This is supported by our finding that EBV DNA was detected in ocular samples from patients with severe intraocular inflammatory disease such as ARN and bacterial or fungal endophthalmitis (see Table 2).

Cytomegalovirus DNA was detected in patients with corneal endotheliitis, anterior uveitis without corneal endothelium edema, and CMV retinitis. Corneal endotheliitis or anterior uveitis was not seen in immunocompromised patients. However, CMV retinitis was seen in immunocompromised patients, such as those with HIV infections. Cytomegalovirus-related anterior uveitis is similar to Posner-Schlossman syndrome, in which whitish, small, mutton-fat keratic precipitates, high intraocular pressure, and mild inflammation

Table 2. Comprehensive Polymerase Chain Reaction Results for Each Infectious Genome in Patients with Uveitis and Endophthalmitis

Infectious Antigens	Clinical Diagnosis	Positive PCR Results*/ Total No. of Patients (Mean Age of Onset [yrs])
HSV-1	Herpetic keratouveitis	1/4† (43)
	Herpetic anterior uveitis	16/76 (51)
	Acute retinal necrosis	1/29 (39)
	Others	0/391 (—)
HSV-2	Acute retinal necrosis	4/29 (28)
	Others	0/471 (—)
VZV	Herpetic keratouveitis	2/4 (61)
	Herpetic anterior uveitis	26/76 (66)
	Acute retinal necrosis	24/29 (51)
	PORN	2/2 (53)
	Others	1/389 (55)
EBV	Idiopathic uveitis	5/107 (60)
	Fungal endophthalmitis	3/11 (69)
	Bacterial endophthalmitis	1/38 (75)
	Acute retinal necrosis (VZV)	3/24 (49)
	Intraocular lymphoma	1/43 (72)
	Others	4/277 (48)
CMV	Corneal endotheliitis	11/12 (67)
	Herpetic anterior uveitis	32/76 (58)
	Cytomegalovirus retinitis	23/23 (57)
	Others	2/389 (52)
HHV-6	Bacterial endophthalmitis	2/38 (71)
	Others	0/462 (—)
HHV-7	—	0/500 (—)
HHV-8	—	0/500 (—)
Toxoplasmosis	Ocular toxoplasmosis	6/9 (55)
	Others	0/491 (—)
Bacteria 16S	Bacterial endophthalmitis	26/38 (64)
	Idiopathic uveitis	3/107 (54)
	Others	4/355 (67)
Fungal 18S/28S	Fungal endophthalmitis	9/11 (61)
	Fungal keratitis	1/1 (55)
	Others	1/488 (65)

CMV = cytomegalovirus; EBV = Epstein-Barr virus; HHV-6 through HHV-8 = human herpes virus types 6 through 8; HSV-1 and HSV-2 = herpes simplex virus types 1 and 2; PCR = polymerase chain reaction; PORN = progressive outer retinal necrosis; VZV = varicella-zoster virus.
*Detection of infectious DNA by multiplex PCR combined with real-time PCR or broad-range real-time PCR.
†In the 4 keratouveitis patients, the PCR system detected HSV-1 DNA in only 1 patient.

Table 3. False-Negative Results for Polymerase Chain Reaction

Clinical Diagnosis	False-Negative Results*
Corneal endotheliitis (cytomegalovirus)	1
Herpetic keratouveitis	1
Herpetic anterior uveitis	2
Ocular toxoplasmosis	3
Bacterial endophthalmitis	12
Fungal endophthalmitis	2

*False-negative results indicate negative polymerase chain reaction results, with a final diagnosis of ocular infection as determined by other examinations, clinical findings, or responses to treatment.

in the anterior chamber are observed.[11,12] In these types of cases, both the retina and fellow eye usually are intact. However, CMV-related corneal endotheliitis exhibits corneal endothelium edema but not anterior uveitis.[12–15] Recently, several investigators have reported finding cases of CMV-associated corneal endotheliitis when using this new PCR technique.[12,15,16] It additionally was reported that this inflammation could be well controlled through the use of antiviral agents.[12–16]

In both our previous and present studies, we observed a few cases with positive HHV-6 results. As reported previously, we also have encountered a patient with apparent severe unilateral panuveitis.[17] After further examination of this particular case, we finally determined the patient had ocular toxocariasis and HHV-6–associated panuveitis. In addition, we also found 2 HHV-6–positive cases with bacterial endophthalmitis in our present study, with neither of the patients found to be immunocompromised. Thus, at the present time there is no conclusive evidence that clarifies whether viral replication of HHV-6 occurs in the eye. Of all of the patients examined in the present study, there were no HHV-7– or HHV-8–positive cases.

This study examined many bacteria-positive endophthalmitis cases. Sample analysis led to the detection of bacterial 16S rDNA in 26 of 38 patients with clinically suspected bacterial endophthalmitis. With the exception of the PCR-negative cases, high bacterial DNA copy numbers were detected in all of these patients. Our broad-range real-time PCR detected bacterial 16S rDNA in samples from 3 patients with idiopathic uveitis, which were false-positive results (Table 4). However, bacteria 16S copy numbers were not very high in these patients. It has been suggested that amplification of bacteria species may occur in patients undergoing long-term steroid treatments. In fact, the 3 cases in our present study all had received subconjunctival injections, systemic steroids, or both over a long period. Other explanations for our present results could be contamination caused by technical errors during the PCR preparation or bacterial exposure that occurred when collecting the samples (e.g., contamination resulting from conjunctival ocular flora present when collecting the ocular sample). Other than these 3 cases, we did not observe any PCR false-positive results resulting from herpes virus, fungi, or parasites.

In this study, we used 2 PCR methods to detect fungal infections, one for fungal 18S and one for 28S rDNA. For the 18S, we designed pan-fungal primers and probes that were complementary to the 18S rRNA sequences present in the *Candida* and *Aspergillus* species.[5] Our PCR system detected 6 *Candida* species, along with 5 *Aspergillus* species. In another study, we used several different primers and probes to detect separately each of these fungal species.[5] Additionally, although our PCR examination was able to detect all species of *Candida* and *Aspergillus* DNA, it did not detect any other fungi DNA. Therefore, we prepared a separate assay that targeted a part of the 28S large subunit rRNA genes for others.[6,18] *Candida* ocular infection is very similar to endogenous endophthalmitis, and in the past, we have encountered some rare *Aspergillus*-positive cases, for example, retinal vasculitis, endogenous endophthalmitis, late postoperative endophthalmitis, and post-traumatic keratitis-associated endophthalmitis. Fungal DNA was detected in 9 of the 11 ocular samples obtained from fungal endophthalmitis patients (Table 2). One fungal keratitis case also had positive results for fungal 28S rDNA in the aqueous humor. These PCR-positive samples all had significantly high copy numbers of *Candida*, *Aspergillus*, or *Cryptococcus* DNA. In 2 patients who were clinically suspected of having *Candida* endophthalmitis, our PCR analysis did not detect any fungal genome in the ocular sample. However, it should be noted that this sample was aqueous humor, and if we had obtained a vitreous sample instead, we might have detected *Candida* DNA because *Candida* endophthalmitis often results from hematogenous dissemination. This finding suggests that the type of sample collected could be very important with regard to the ability to make an accurate diagnosis.

In our bacterial 16S PCR study, we found false-negative results in 12 of the 38 samples obtained from clinically suspected bacterial endophthalmitis patients (Table 3). The false-negative results were defined as being negative for PCR even though there was a clinically suspected bacterial infection, for example, culture positive, having an inflammation that was well-controlled by antibiotics, or both. Once again, it is necessary to consider how the samples were actually obtained in these cases. Bacterial 16S rDNA was not detected in a few of the endogenous bacterial endophthalmitis patients. However, because endogenous endophthalmitis results from hematogenous dissemination, it might have been possible to detect bacterial genome if we had collected vitreous samples. Although the proper DNA extraction procedure required for verifying bacterial infec-

Table 4. False-Positive Results for Polymerase Chain Reaction

Polymerase Chain Reaction for Infectious Antigens	False-Positive Results*
Bacteria 16S	3

*False-positive results indicate positive polymerase chain reaction results, with a final diagnosis of clinically noninfectious disease. These patients with bacteria 16S false-positive resuts ultimately were diagnosed with idiopathic uveitis.

tion by PCR remains controversial, we have attempted to use various approaches for the DNA extraction that will upregulate the PCR sensitivity. In general, a bactericidal enzyme pretreatment (e.g., lysozyme pretreatment) is required for bacterial cell wall destruction, and several investigators have reported previously finding lysozyme resistance in gram-negative and gram-positive bacteria species.[19,20] However, we did not pretreat any of our samples with enzyme because of the limited amount of sample that was available and the fact that our PCR examination included other infectious agents, such as viruses, fungi, and parasites. Therefore, it possible that bacterial 16S rDNA might not have been detected in a few of the endogenous bacterial endophthalmitis patients because of difficulties in collecting samples from patients with infectious agglomeration.

In conclusion, our results indicate that a comprehensive PCR system can be used to verify ocular disease diagnoses definitively. Furthermore, this PCR system also is able to exclude ocular infections as the potential cause of ocular disorders and, based on the confidence of the diagnosis, can be used to help design appropriate early treatments for ocular disease. Because it is important to be able to exclude noninfectious uveitis or endophthalmitis, the PCR-negative results can help to simplify the clinical workups in these cases. Additionally, because PCR examinations can be used to exclude infectious agents, this makes it easier to determine which cases are applicable for use of steroids. Although unfortunately this laboratory approach is not commercially available at the present time, we currently are pursing plans to create a simple examination kit that can be used for ocular infectious diseases in the near future.

References

1. Sugita S, Shimizu N, Watanabe K, et al. Diagnosis of bacterial endophthalmitis by broad-range quantitative PCR. Br J Ophthalmol 2011;95:345–9.
2. Sugita S, Shimizu N, Watanabe K, et al. Use of multiplex PCR and real-time PCR to detect human herpes virus genome in ocular fluids of patients with uveitis. Br J Ophthalmol 2008; 92:928–32.
3. Sugita S, Iwanaga Y, Kawaguchi T, et al. Detection of herpesvirus genome by multiplex polymerase chain reaction (PCR) and real-time PCR in ocular fluids of patients with acute retinal necrosis. Nippon Ganka Gakkai Zasshi 2008;112: 30–8.
4. Sugita S, Ogawa M, Inoue S, et al. Diagnosis of ocular toxoplasmosis by two polymerase chain reaction (PCR) examinations: qualitative multiplex and quantitative real-time. Jpn J Ophthalmol 2011;55:495–501.
5. Sugita S, Kamoi K, Ogawa M, et al. Detection of Candida and Aspergillus species DNA using broad-range real-time PCR for fungal endophthalmitis. Graefes Arch Clin Exp Ophthalmol 2012;250:391–8.
6. Ogawa M, Sugita S, Watanabe K, et al. Novel diagnosis of fungal endophthalmitis by broad-range real-time PCR detection of fungal 28S ribosomal DNA. Graefes Arch Clin Exp Ophthalmol 2012;250:1877–83.
7. Kido S, Sugita S, Horie S, et al. Association of varicella zoster virus load in the aqueous humor with clinical manifestations of anterior uveitis in herpes zoster ophthalmicus and zoster sine herpete. Br J Ophthalmol 2008;92:505–8.
8. Yamamoto S, Sugita S, Sugamoto Y, et al. Quantitative PCR for the detection of genomic DNA of Epstein-Barr virus in ocular fluids of patients with uveitis. Jpn J Ophthalmol 2008; 52:463–7.
9. Ongkosuwito JV, Van der Lelij A, Bruinenberg M, et al. Increased presence of Epstein-Barr virus DNA in ocular fluid samples from HIV negative immunocompromised patients with uveitis. Br J Ophthalmol 1998;82:245–51.
10. Chodosh J, Gan Y-J, Sixbey JW. Detection of Epstein-Barr virus genome in ocular tissues. Ophthalmology 1994;104: 705–8.
11. Kawaguchi T, Sugita S, Shimizu N, et al. Kinetics of aqueous flare, intraocular pressure and virus-DNA copies in a patient with cytomegalovirus iridocyclitis without retinitis. Int Ophthalmol 2007;27:383–6.
12. Miyanaga M, Sugita S, Shimizu N, et al. A significant association of viral loads with corneal endothelial cell damage in cytomegalovirus anterior uveitis. Br J Ophthalmol 2010;94: 336–40.
13. de Schryver I, Rozenberg F, Cassoux N, et al. Diagnosis and treatment of cytomegalovirus iridocyclitis without retinal necrosis. Br J Ophthalmol 2006;90:852–5.
14. Chee SP, Jap A. Presumed Fuchs heterochromic iridocyclitis and Posner-Schlossman syndrome: comparison of cytomegalovirus-positive and negative eyes. Am J Ophthalmol 2008;146: 883–9.
15. Chee SP, Bacsal K, Jap A, et al. Corneal endotheliitis associated with evidence of cytomegalovirus infection. Ophthalmology 2007;114:798–803.
16. Koizumi N, Suzuki T, Uno T, et al. Cytomegalovirus as an etiologic factor in corneal endotheliitis. Ophthalmology 2008; 115:292–7.
17. Sugita S, Shimizu N, Kawaguchi T, et al. Identification of human herpesvirus 6 in a patient with severe unilateral panuveitis. Arch Ophthalmol 2007;125:1426–7.
18. Vollmer T, Störmer M, Kleesiek K, et al. Evaluation of novel broad-range real-time PCR assay for rapid detection of human pathogenic fungi in various clinical specimens. J Clin Microbiol 2008;46:1919–26.
19. Callewaert L, Aertsen A, Deckers D, et al. A new family of lysozyme inhibitors contributing to lysozyme tolerance in gram-negative bacteria. PLoS Pathog 2008;4:e1000019.
20. Davis KM, Akinbi HT, Standish AJ, et al. Resistance to mucosal lysozyme compensates for the fitness deficit of peptidoglycan modifications by Streptococcus pneumoniae. PLoS Pathog 2008;4:e1000241.

Footnotes and Financial Disclosures

Originally received: September 26, 2012.
Final revision: February 18, 2013.
Accepted: February 18, 2013.
Available online: May 7, 2013. Manuscript no. 2012-1475.

[1] Department of Ophthalmology & Visual Science, Tokyo Medical and Dental University, Tokyo, Japan.

[2] Laboratory for Retinal Regeneration, RIKEN Center for Developmental Biology, Kobe, Japan.

[3] Department of Virology, Medical Research Institute, Tokyo Medical and Dental University, Tokyo, Japan.

[4] Center for Cell Therapy, Tokyo Medical and Dental University, Tokyo, Japan.

[5] Department of Ophthalmology, Osaka Koseinennkinn Hospital, Osaka, Japan.

[6] Department of Ophthalmology, Osaka University Graduate School of Medicine, Osaka, Japan.

[7] Department of Ophthalmology, Kyoto Prefectural University of Medicine, Kyoto, Japan.

[8] Department of Ophthalmology, Kyushu University Graduate School of Medical Sciences, Fukuoka, Japan.

[9] Department of Ophthalmology, Tokyo Medical University, Tokyo, Japan.

[10] Department of Ophthalmology, Yamaguchi University Graduate School of Medicine, Yamaguchi, Japan.

[11] Department of Ophthalmology, National Defense Medical College, Tokyo, Japan.

Financial Disclosure(s):
The author(s) have no proprietary or commercial interest in any materials discussed in this article.

Supported by a Comprehensive Research on Disability, Health and Welfare grant, along with a Health and Labour Sciences Research Grant from the Ministry of Health, Labour and Welfare, Tokyo, Japan.

Correspondence:
Sunao Sugita, MD, PhD, Laboratory for Retinal Regeneration, RIKEN Center for Developmental Biology, 2-2-3 Minatojima-minamimachi, Chuo-ku, Kobe 650-0047, Japan. E-mail: sunaoph@cdb.riken.jp.

Cancer Science
The official journal of the Japanese Cancer Association JCA

Artemis-dependent DNA double-strand break formation at stalled replication forks

Junya Unno,[1,2] Masatoshi Takagi,[1,8] Jinhua Piao,[1] Masataka Sugimoto,[3] Fumiko Honda,[1] Daisuke Maeda,[4,5] Mitsuko Masutani,[4,5] Tohru Kiyono,[6] Fumiaki Watanabe,[1] Tomohiro Morio,[1] Hirobumi Teraoka[7] and Shuki Mizutani[1,8]

[1]Department of Pediatrics and Developmental Biology, Graduate School of Medicine, Tokyo Medical and Dental University, Tokyo; [2]Laboratory of DNA damage signaling, Department of Late Effect Studies, Radiation Biology Center, Kyoto University, Kyoto; [3]Section of Biochemistry, Department of Mechanism of Aging, National Institute for Longevity Sciences, National Center for Geriatrics and Gerontology, Aichi; [4]Biochemistry Division; [5]ADP-ribosylation in Oncology Project; [6]Virology Division, National Cancer Center Research Institute, Tokyo; [7]Department of Pathological Biochemistry, Medical Research Institute, Tokyo Medical and Dental University, Tokyo, Japan

(Received January 22, 2013/Revised February 26, 2013/Accepted March 2, 2013/Accepted manuscript online March 6, 2013/Article first published online April 15, 2013)

Stalled replication forks undergo DNA double-strand breaks (DSBs) under certain conditions. However, the precise mechanism underlying DSB induction and the cellular response to persistent replication fork stalling are not fully understood. Here we show that, in response to hydroxyurea exposure, DSBs are generated in an Artemis nuclease-dependent manner following prolonged stalling with subsequent activation of the ataxia–telangiectasia mutated (ATM) signaling pathway. The kinase activity of the catalytic subunit of the DNA-dependent protein kinase, a prerequisite for stimulation of the endonuclease activity of Artemis, is also required for DSB generation and subsequent ATM activation. Our findings indicate a novel function of Artemis as a molecular switch that converts stalled replication forks harboring single-stranded gap DNA lesions into DSBs, thereby activating the ATM signaling pathway following prolonged replication fork stalling. (*Cancer Sci* 2013; 104: 703–710)

DNA replication is a crucial phase in cell proliferation and is always accompanied by the possibility of generating DNA irregularities. To prevent the disruption of genome integrity during replication by exogenous or endogenous stresses, replication fork progression is precisely regulated and monitored by the replication checkpoint.[1] This machinery is one of the targets for cancer chemotherapy such as alkylating agents or inhibitors of ribonucleotide reductase, which cause an imbalance in the deoxynucleotide triphosphate pool. Stalled replication forks lead to the production of ssDNA lesions including ssDNA gaps, which in some cases are converted to DSBs, an event termed replication fork collapse, by a mechanism in which some nucleases play a key role. Double-strand breaks (DSB) thus generated must be monitored and resolved by DNA damage response mechanisms to maintain genome integrity.

Ataxia–telangiectasia mutated (ATM) is mainly activated by DSBs and recruited to damage sites by the Mre11-Rad50-NBS1 complex.[2] Ataxia-telangiectasia mutated (ATM) exists as an inactive dimer and undergoes autophosphorylation, which triggers monomerization and activation.[3] Another damage-response protein, the ATR–ATR-interacting protein complex, is principally activated by RPA-coated ssDNA regions thatarise at stalled replication forks or during the processing of bulky lesions such as UV photoproducts and DSBs in S/G_2 phases.[4] Once ATM and ATR are activated by DNA lesions, they cooperatively stimulate DNA damage checkpoint pathways through the phosphorylation of numerous substrates, leading to cell cycle arrest, apoptosis, DNA repair, or cell senescence.[5]

The Artemis nuclease is mutated in individuals with RS-SCID. *In vitro*, in the presence of ATP and DNA-PK composed of DNA-PKcs (officially known as protein kinase, DNA-activated, catalytic polypeptide [PRKDC]) and the Ku70/80 heterodimer, Artemis acquires DNA endonuclease activity that specifically targets ssDNA–dsDNA junctions including 5′- or 3′- overhangs, hairpins, and gaps.[6,7] Autophosphorylation of DNA-PKcs at the ABCDE cluster (Thr2609, Ser2612, Thr2620, Ser2624, Thr2638, and Thr2647) is essential for Artemis endonuclease activity.[6] Through its endonuclease activity, Artemis contributes to the repair of a fraction of DSBs (~10%) induced by ionizing radiation *in vivo*, suggesting that it processes the ends of DSBs that are refractory to repair by core non-homologous end joining factors such as Ku70, Ku80, XRCC4, and DNA ligase IV.[8]

Here, we show that the ATR signaling pathway is activated at an early phase of replication fork stalling, and that extensive activation of the ATM signaling pathway is triggered by the generation of DSBs by Artemis nuclease following prolonged replication fork stalling. DNA-PKcs kinase activity is also required for this DSB generation and subsequent ATM activation. Artemis-deficient fibroblasts show resistance to HU. From these results, we propose that the Artemis/DNA-PK machinery plays an essential role in the mechanism that responds to prolonged replication fork stalling by HU.

Materials and Methods

Cells. HeLa, U2OS, M059J, and M059K were obtained from ATCC (Manassas, VA, USA). Human telomerase reverse transcriptase immortalized human diploid fibroblasts (HDF2/326) were described previously.[9]

Immunoblotting and immunofluorescence. Immunoblotting and immunofluorescence were carried out using standard methods. Details of the experimental procedure are also provided in Document S1.

Results

Activation of DNA damage response by HU. To obtain insights into the mechanism by which stalled DNA replication forks are converted to DSBs under certain conditions, we measured the phosphorylation of various ATM/ATR substrates to monitor the status of DNA damage checkpoint activation in response to HU. To assess the effect of HU treatment only in S phase, we synchronized HeLa cells at the G_1-S boundary with a double thymidine block, then released them into S phase for 1 h prior to HU exposure (Fig. S1a). As shown in Figure 1(a), Chk1 Ser345 and NBS1 Ser343 were strongly

[8]To whom correspondence should be addressed.
E-mails: m.takagi.ped@tmd.ac.jp or smizutani.ped@tmd.ac.jp

doi: 10.1111/cas.12144

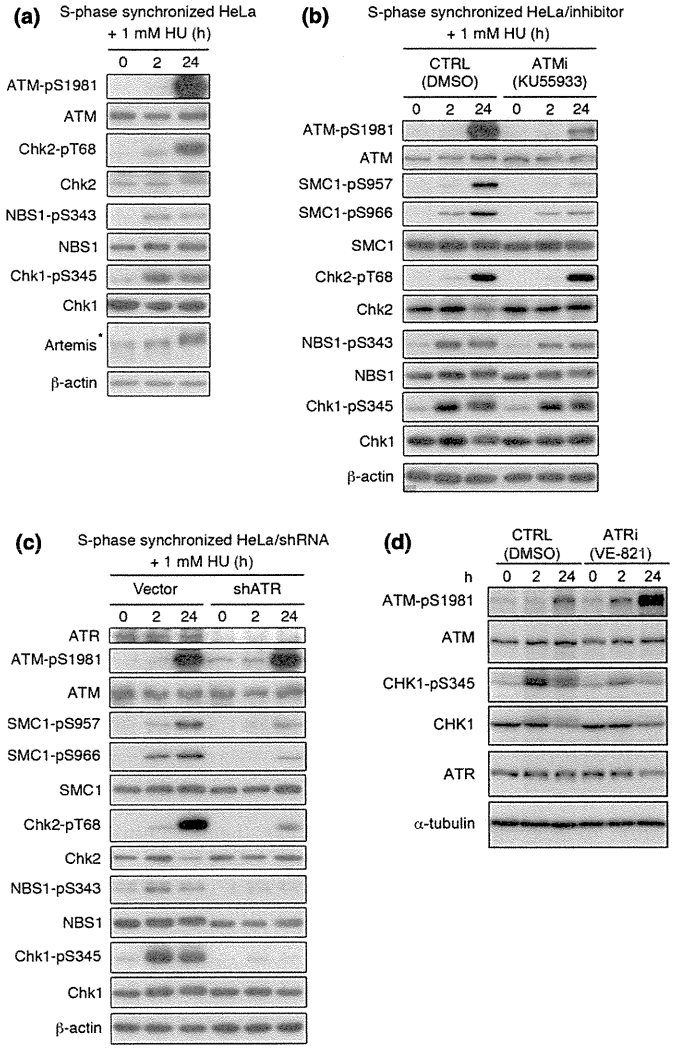

Fig. 1. Ataxia–telangiectasia and RAD3-related (ATR) and ataxia–telangiectasia mutated (ATM) pathways are differentially activated by exposure to hydroxyurea (HU). (a) S-phase synchronized HeLa cells were treated with 1 mM HU 1 h after release from double thymidine block. Cell extracts from the indicated time points were immunoblotted with the indicated antibodies. *Hypersphosphorylated form of Artemis. (b) Synchronized HeLa cells were treated with 1 mM HU 1 h after release from double thymidine blockwith or without ATM-specific inhibitor KU55933 (10 μM). (c) HeLa cells were transfected with shATR-expressing construct or mock vector. The cells were synchronized 24 h after transfection. One hour after release from double thymidine block, cells were treated with 1 mM HU for 2 or 24 h. (d) Synchronized HeLa cells were treated with 1 mM HU 1 h after release from double thymidine blockwith or without ATR-specific inhibitor VE-821 (10 μM). CTRL, control.

phosphorylated after a 2-h exposure to HU. Phosphorylation of ATM at Ser1981 was weakly detectable at 2 h and significantly enhanced after 24 h continuous exposure to HU. Chk2 Thr68 was phosphorylated in parallel with ATM phosphorylation. The activation of the ATM signaling pathway after HU was confirmed by addition of the ATM specific inhibitor KU55933 that attenuated ATM phosphorylation at Ser1981 and SMC1 phosphorylation at Ser957 and Ser966 after HU exposure (Fig. 1b). In contrast, phosphorylation of Chk2, NBS1, and Chk1 was not inhibited by treatment with KU55933 (Fig. 1b, Fig. S1b). As Chk2 was phosphorylated even in ATM-inhibited cells, Chk2 might be phosphorylated by ATR or DNA-PKcs. This result indicates that ATM phosphorylation after HU exposure for 24 h is the result of autophosphorylation, and that ATM preferentially phosphorylates SMC1 after HU exposure.

Previously, phosphorylation of ATM after replication fork stalling has been reported to be dependent on ATR activation.[10] Hence, we investigated whether DNA damage signaling caused by prolonged HU exposure was ATR-dependent using ATR knockdown cells produced with an ATR-specific shRNA[11] (Fig. 1c) or siRNA to target a distinct ATR sequence (Fig. S1c). Increased ATM autophosphorylation was observed after ATR knockdown even in the absence of HU, presumably due to an increase in DSBs or genomic instability caused by ATR depletion.[12] After 2 h exposure to HU, a slightly elevated level of ATM phosphorylation was observed in both cells. After 24 h exposure to HU, ATM was strongly autophosphorylated even in ATR knockdown cells. The ATR knockdown strikingly reduced Chk1 and NBS1 phosphorylation, and partly attenuated Chk2 and SMC1 phosphorylation after both 2 h and 24 h exposure to HU. Although NBS1, Chk2, and SMC1 are well-known ATM targets, NBS1, Chk2, and SMC1 were also phosphorylated in an ATR-dependent manner after HU treatment (Fig. 1c, Fig. S1d). Treatment with the ATR inhibitor VE-821 also represented the siRNA-dependent ATR knockdown experiment (Fig. 1d). These data are consistent with previous reports showing that Chk1, NBS1, and SMC1 are phosphorylated in an ATR-dependent manner after HU or UV exposure[13,14] and that Chk2 can be phosphorylated by ATR *in vitro*.[15] From these results, we concluded that ATM is activated in an ATR-independent manner after prolonged exposure to HU.

Long continuous HU exposure induces DSB. To investigate the precise mechanisms underlying the activation of the ATM signaling pathway after prolonged HU exposure, the concomitant formation of foci of γH2AX, which is indicative of stalled replication forks and DNA DSBs,[16,17] and RPA2, a hallmark of ssDNA lesions, was investigated by immunofluorescence microscopy. γH2AX and RPA2 foci were detectable after a 2-h exposure to HU, although these signals were relatively smaller and weaker than those observed after 24 h exposure. At the 2 h time point, most γH2AX foci colocalized with RPA2 foci (Fig. 2a,b,Fig. S2a). After 24 h HU treatment, γH2AX and RPA2 foci were more intense and granular. Interestingly, although both foci were detectable, most γH2AX foci no longer colocalized with RPA2 foci at this time point (Fig. 2a,b, Fig. S2a,b). After HU treatment, pS1981 phosphorylated ATM formed foci colocalizing with γH2AX in HeLa cells (Fig. S3a). After HU treatment for 24 h, pS1981 phosphorylated ATM was detected as clearly larger foci, and some of these were independent from RPA2 foci in wild-type derived control fibroblasts (WT fibroblasts). However, ATM-pS1981 foci, consisting of weakly stained fine granules, colocalized with RPA2 foci in Artemis-mutated RS-SCID derived AV2/326 cells (Artemis-deficient fibroblasts) (Fig. S3b). These results are compatible with the interpretation that short-term HU exposure causes replication fork arrest and prolonged HU exposure induces DSB, consistent with a previous report indicating the existence of DSB after prolonged HU treatment.[18] To detect DSBs directly, DNA fragmentations after HU exposure were investigated by PFGE. After more than 12 h of HU exposure, increasing amounts of DSBs were clearly generated (Fig. 2c,d). Collectively, observations from Figures 1 and 2 support a two-step model for the activation of DNA damage checkpoints in response to HU-induced replication fork stalling: the primary activation of the ATR signaling as an early phase response to stalled replication fork and the secondary activation of the ATM signaling pathway as a late response to DSB.

Artemis-dependent DSBs activate ATM signaling. Because the relationship between prolonged replication fork stalling and DSB generation has not been precisely clarified, we sought to determine the key factor for DSB formation under these

doi: 10.1111/cas.12144

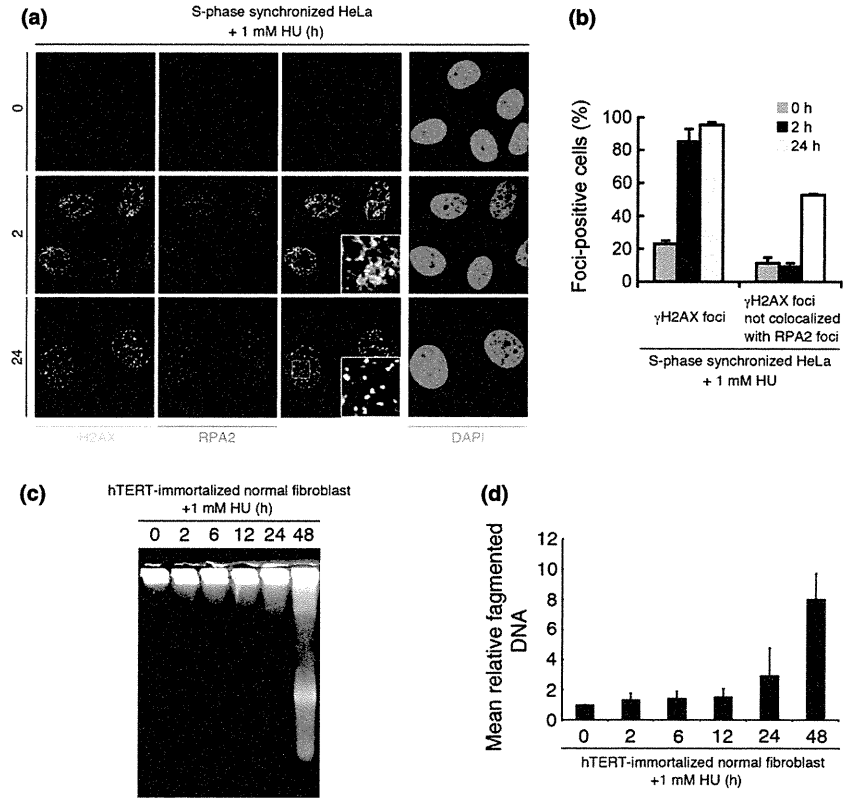

Fig. 2. Short-term hydroxyurea (HU) exposure causes replication fork arrest and 24 h continuous HU exposure induces double-strand breaks (DSB). (a) HeLa cells were synchronized at S phase and treated with 1 mM HU for 2 h or 24 h. Cells were fixed and stained with anti-phosphorylated histone H2AX (γH2AX) (Ser139) and anti-replication protein A2(RPA2) antibodies. (b) More than 100 cells were counted, and the percentage showing >10 γH2AX foci or >4 γH2AX foci not colocalized with RPA2 foci was determined. Data represent the mean ± SEM from three independent experiments. (c) Human telomerase reverse transcriptase (hTERT)-immortalized normal human fibroblasts (HDF2/326) were treated with 1 mM HU for indicated times. Cells were analyzed by pulse field gel electrophoresis (PFGE). (d) Mean relative fragmented DNA (1 = the fraction of DNA released from the gel plug in untreated fibroblasts) from (c) was calculated, and data are shown in the bar graph. Data represent the mean ± SEM from two independent experiments.

conditions. The recruitment of endonuclease(s) to the ssDNA–dsDNA junction, a structure that arises in replication fork stalling, is likely to lead to the generation of DSBs.[16,19] Since the Artemis nuclease is known to process ssDNA–dsDNA junctions *in vitro*,[6,7] we hypothesized that processing of stalled replication forks by the Artemis nuclease leads to generation of DSBs after prolonged HU exposure. To test this possibility, we investigated HU-induced DSBs using WT and Artemis-deficient hTERT-immortalized fibroblasts derived from RS-SCID patients. Pulse field gel electrophoresis (PFGE) showed a lower level of dose-dependent generation of DSBs in Artemis-deficient fibroblasts compared to WT fibroblasts after HU exposure (Fig. 3). Camptothecin treatment was used as a positive control for replication-associated DSB,[11,20] showing no significant difference of DSBs in cells with or without Artemis (Fig. S4a, b). Identical results were obtained with the neutral comet assay, which detects DSBs at the single-cell level, confirming our PFGE data (Fig. S4c,d). These data suggest that DSB generation after prolonged HU exposure is Artemis-dependent.

We also investigated whether the extent of DSB formation induced by HU exposure correlates with the level of DNA damage checkpoint activation. Interestingly, Artemis-deficient fibroblasts treated with HU for 24 h showed attenuated activation of ATM signaling compared to WT fibroblasts (Fig. 4a). To consolidate this finding, we also investigated the effect of Artemis knockdown in HeLa cells using two independent shRNA constructs. These transfectants showed cell cycle kinetics similar to control shRNA-transfected cells (Fig. S5). Artemis knockdown HeLa cells thus generated showed attenuated activation of the ATM signaling pathway after 24 h HU exposure; in contrast, Chk1 phosphorylation levels were unchanged (Fig. 4b). RPA2 was hyperphosphorylated after only 24 h of treatment with 1 mM HU in Artemis-competent cells, as previously described.[11] Interestingly, hyperphosphorylation of RPA2 was attenuated in Artemis-deficient fibroblasts. After DNA damage, ATM, ATR, and DNA-PK dependent phosphorylation of RPA2 plays a key role in replication checkpoint activation. It has been reported hyperphosphorylated RPA2 associates with ssDNA and recombinase protein Rad51 in response to replication arrest by HU treatment and is critical for Rad51 recruitment and homologous recombination-mediated repair.[21] Artemis-deficient cells may also show homologous recombination-mediated DNA repair defect (Fig 4c,d).

To address the functional importance of Artemis nuclease activity, we introduced WT or nuclease dead construct (H254A; histidine to alanine substitution on amino acid 254) of Artemis into Artemis-deficient fibroblasts. As is shown in Figure 4(e), the Artemis nuclease-dead mutant did not promote efficient activation of ATM signaling after HU treatment. This was in contrast to WT transfectant which efficiently restored ATM activation. Chk1 phosphorylation was indistinguishable between the cells expressing WT and nuclease-dead mutant Artemis. These results are in accord with the interpretation that the nuclease activity of Artemis plays a critical role in the generation of DSBs when replication fork stalling is prolonged by long exposure to HU, and that DSBs, thus generated, lead to activation of the ATM-dependent DNA damage response pathway.

DNA-dependent protein kinase (DNA-PK) is activated by replication fork stalling. *In vitro*, Artemis endonuclease activity is controlled by DNA-PKcs autophosphorylation at the ABCDE cluster.[6] Thus, we investigated whether the kinase activity of DNA-PKcs is involved in Artemis-dependent DSB formation and subsequent ATM activation following prolonged HU exposure. To gain direct evidence for the activation of DNA-PKcs, we monitored its autophosphorylation at Ser2056 and/or Thr2609, which have been reported to be essential for DNA-PKcs function.[22,23] A low level of DNA-PKcs Ser2056 phosphorylation was detected after 2 h of HU exposure, which increased after 24 h HU exposure (Fig. 5a, Fig. S6a). Immunofluorescence examination using a phospho-specific antibody against Thr2609 of DNA-PKcs showed similar results in S-phase synchronized HeLa cells, in which we observed small

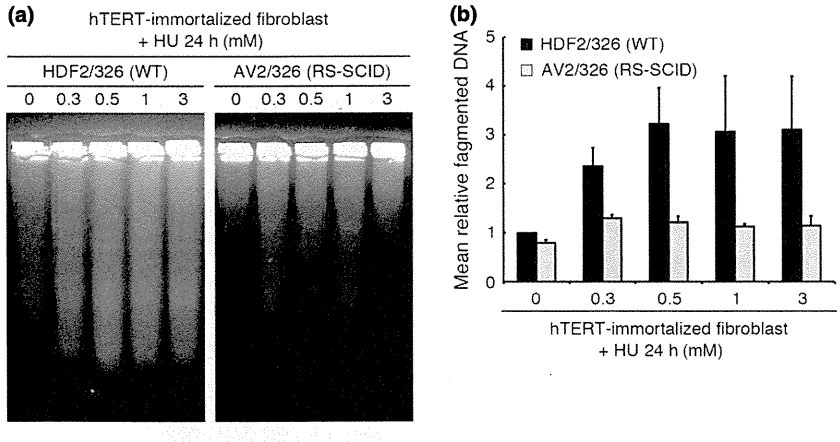

Fig. 3. Double-strand breaks (DSB) generation after replication fork stalling is Artemis-dependent. (a) Human telomerase reverse transcriptase (hTERT)-immortalized normal (HDF2/326;WT) and Artemis-deficient (AV2/326; radiosensitive severe combined immunodeficiency [RS-SCID]) human fibroblasts were treated with the indicated doses of hydroxyurea (HU) for 24 h. Cells were analyzed by pulse field gel electrophoresis (PFGE). (b) Mean relative fragmented DNA (1 = the fraction of DNA released from the gel plug in untreated fibroblasts) from (a) was calculated, and data are shown in the bar graph. Data represent the mean ± SEM from two independent experiments.

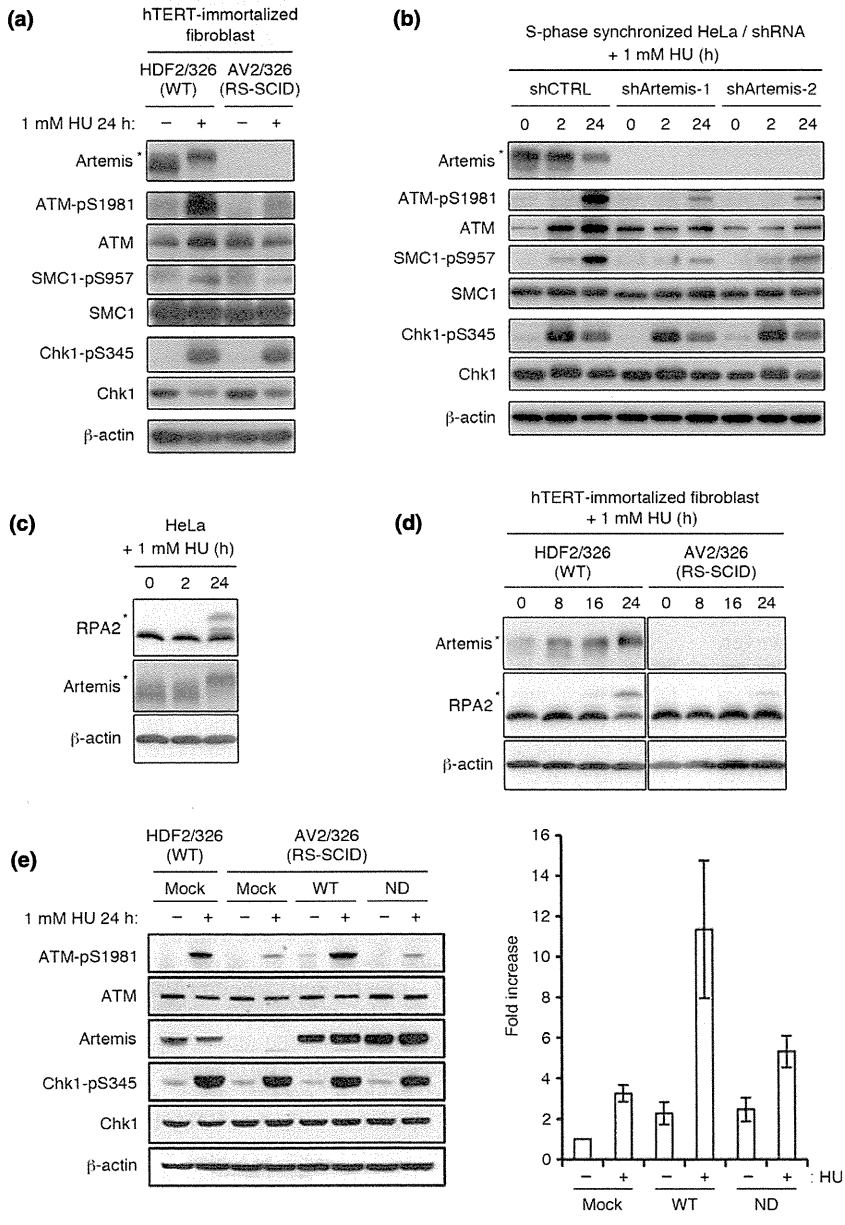

Fig. 4. Activation of the ataxia–telangiectasia mutated (ATM) signaling pathway is Artemis-dependent. (a) HDF2/326 and AV2/326 (radiosensitive severe combined immunodeficiency [RS-SCID] human fibroblasts were treated with 1 mM hydroxyurea (HU) for 24 h. Cell extracts were immunoblotted with the indicated antibodies. (b) HeLa cells were transfected with a control (shCTRL) or two types of shArtemis-expressing construct. Cells were synchronized 24 h after transfection. One hour after release, the cells were treated with 1 mM HU for 2 h or 24 h, and cell extracts were immunoblotted. (c) HeLa cells were treated with 1 mU HU and RPA2 phosphorylation status was determined by Western blotting. (d) Western blot analysis of RPA2 phosphorylation status in HDF2/326 and AV2/326 human fibroblasts. (e) HDF2/326 and AV2/326 human fibroblasts were infected with mock or Artemis WT or H254A nuclease dead mutant (ND). Cells were treated with 1 mM HU for 24 h and subjected to Western blot analysis. Right graph indicates relative ATM phosphorylation standardized to 1 as the base level of mock transduced Artemis-deficient fibroblasts before HU treatment. Data represent the mean ± SEM from three independent experiments. hTERT, human telomerase reverse transcriptase. *Hypersphosphorylated form of Artemis or RPA2.

foci of phospho-DNA-PKcs after a 2 h HU exposure and an increased number and intensity of foci after 24 h HU exposure. These phospho-DNA-PKcs foci colocalized with RPA2 foci following 2 h exposure to HU and remained colocalized even after 24 h exposure (Fig. 5b, Fig. S6b), indicating that DNA-PKcs is activated on stalled replication forks.

Because DNA-PK has been shown to bind to dsDNA ends and is believed to require dsDNA ends for its activation,[24,25]

doi: 10.1111/cas.12144

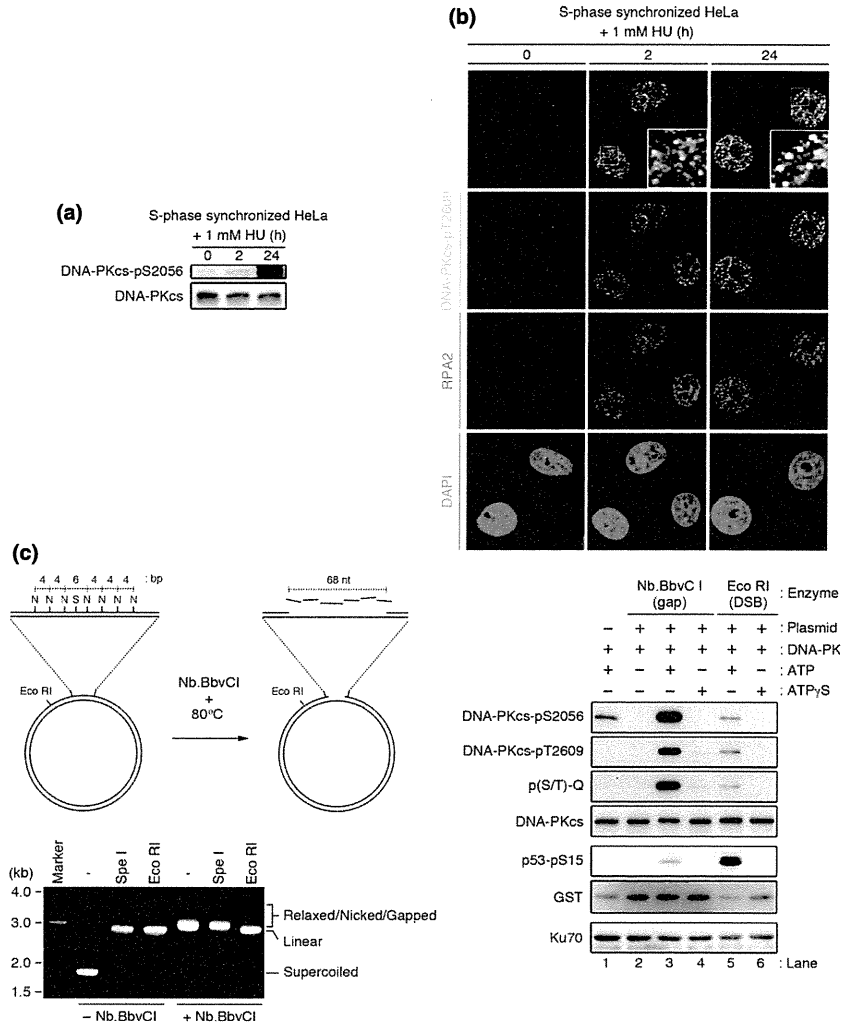

Fig. 5. Activation of catalytic subunit of DNA-dependent protein kinase (DNA-PKcs) by stalled replication forks after treatment with hydroxyurea (HU). (a) S-phase synchronized HeLa cells were treated with 1 mM HU 1 h after release from double thymidine block. Cell extracts from the indicated time points were immunoblotted with an anti-phospho-DNA-PKcs (Ser2056) and generic DNA-PKcs antibody. (b) Same as in (a), cells were stained with anti-phospho-DNA-PKcs (Thr2609) and anti-RPA2 antibodies. (c) Left panel, generation of a single-stranded gap region on pG68 plasmid. Nb.BbvCI digestion generated a nick on the plasmid, and subsequent heat denaturation released DNA fragments. N, Nb.BbvCI site; S, SpeI site. Lower panel, restriction digestion analysis with indicated enzymes. Nb.BbvCI-treated pG68 plasmid was resistant to SpeI digestion (different mobility from EcoRI digestion), indicating the existence of a single-stranded DNA gap in the plasmid. The DNA-PK holoenzyme is activated by a plasmid containing a single-stranded gap DNA *in vitro*. The reaction was analyzed, followed by SDS-PAGE and immunoblotting using indicated antibodies.

our results in Figure 5(a,b) are difficult to interpret. However, several reports have suggested that DNA-PKcs exerts kinase activity at ssDNA–dsDNA junctions in the absence of a dsDNA end *in vitro*.[25,26] The Ku heterodimer is also able to bind to ssDNA–dsDNA junctions *in vitro*.[27] Therefore, we monitored autophosphorylation of DNA-PKcs (Ser2056, Thr2609, and phospho-(S/T)Q) and phosphorylation of p53 peptide (amino acids 1–100) as an indicator of kinase activity to investigate whether ssDNA gaps could activate DNA-PK. To activate DNA-PK, we used a pG68 plasmid carrying an array of seven Nb.BbvCI and one Eco RI sites.[28] Nb.BbvCI or EcoRI treatment created a single-stranded gap DNA region or dsDNA ends on the plasmid, respectively (Fig. 5c). These enzyme-treated plasmids facilitated autophosphorylation of DNA-PKcs only in the presence of ATP (Fig. 5c, lanes 3,5), as assays performed without ATP or with non-hydrolysable ATPγS were unable to support DNA-PKcs autophosphorylation (Fig. 5c, lanes 2,4,6). p53 peptide was preferentially phosphorylated in the presence of dsDNA end than single-stranded gap DNA, which is in accordance with the results of previous studies that used oligonucleotide as activating DNA.[25–27] Thus, our *in vitro* findings strongly support the interpretation that HU-induced stalled replication forks activate DNA-PKcs *in cellulo*. Therefore, we can conclude that DNA-PKcs is activated on stalled replication forks (which are presumably single-stranded gap DNA lesions harboring ssDNA–dsDNA junctions) by HU exposure.

Next, we addressed the relationship between activation of DNA-PKcs and Artemis *in cellulo*. Autophosphorylation of DNA-PKcs was detected in WT and Artemis-deficient fibroblasts following exposure to HU (Fig. S6c). Immunofluorescence microscopy revealed that autophosphorylated DNA-PKcs (Thr2609) foci were also formed in the absence of Artemis after HU exposure, with an almost equal percentage of foci-positive cells in WT and Artemis-deficient fibroblasts (Fig. S6d). These results suggest that the activation of DNA-PKcs by HU treatment is not Artemis-dependent.

Catalytic subunit of DNA-dependent protein kinase (DNA-PKcs) is required for HU-induced DSB formation. Since the inhibition of DNA-PKcs kinase activity affects the endonuclease activity of Artemis,[6] we investigated whether suppression of DNA-PKcs kinase activity by the specific inhibitor NU7026 affects DSB formation and subsequent ATM activation. Indeed, NU7026 attenuated DSB formation measured by PFGE (Fig. 6a,b) and neutral comet assay (Fig. S7a,b). Identical results were obtained with the DNA-PKcs-deficient human glioma cell line M059J and parental control M059K by neutral comet assay (Fig. S7c,d). NU7026 attenuated subsequent activation of ATM signaling after 24 h HU exposure (Fig. 6c). Taken together, these results suggest that DNA-PKcs is initially autophosphorylated in response to single-stranded gap DNA lesions at stalled replication forks, which leads to DSB induction mediated by Artemis nuclease and subsequent activation of the ATM signaling pathway.

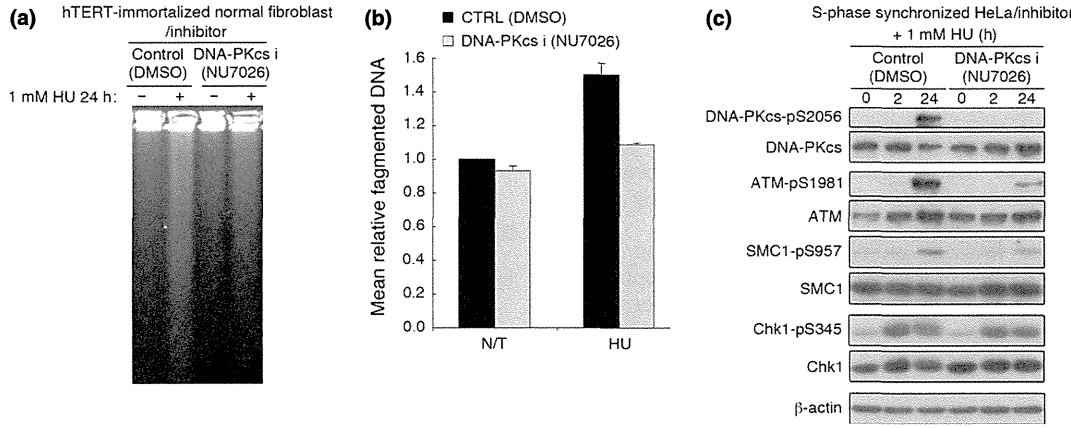

Fig. 6. Double-strand breaks (DSB) generation and ataxia–telangiectasia mutatedactivation (ATM) activation following prolonged replication fork stalling are dependent on catalytic subunit of DNA-dependent protein kinase (DNA-PKcs) activity. (a) Normal human fibroblasts (HDF2/326) were pretreated with DMSO or 10 μM NU7026 for 1 h, and treated with 1 mM HU for 24 h in the presence or absence (DMSO) of NU7026 (10 μM). Cells were analyzed by pulse field gel electrophoresis (PFGE). (b) Mean relative fragmented DNA (1 = the average of the fraction of DNA released from the gel plug in untreated control) from (a) was calculated, and data are shown in the bar graph. Data represent the mean ± SEM from two independent experiments. (c) S-phase synchronized HeLa cells were treated with 1 mM HU 1 h after release from double thymidine block with DMSO or NU7026 (10 μM). Cell extracts from the indicated time points were immunoblottedwith the indicated antibodies.

Discussion

We revealed that the Artemis/DNA-PK machinery plays a critical role in generating DSBs after prolonged replication fork stalling by continuous HU exposure. Involvement of some nucleases has been speculated. Recently, the endonuclease Mus81 was shown to be involved in DSB formation after prolonged inhibition of DNA replication by HU and aphidicolin in mouse embryonic stem cells.[19] Mus81 was also shown to interact with human Apollo/SNM1B, a member of the SNM1 nuclease family characterized by the presence of a metallo-β-lactamase domain, and they have been speculated to work cooperatively for DSB formation after replication stress.[29] Because Artemis/SNM1C is also a member of the SNM1 nuclease family, we hypothesized that, like Apollo/SNM1B, Artemis/SMN1C also works cooperatively with Mus81. However, Artemis and Mus81 did not associate with each other before or after HU exposure (data not shown), suggesting that these proteins might function independently against different targets/substrates. For example, Artemis can cleave hairpin or bubble structures, but Mus81 does not process these structures.[30]

After replication fork stalling, secondary structures such as hairpins, stem-loops/bubbles, or similar structures might be formed on ssDNA gaps.[31,32] There is a strong possibility that these secondary structures activate DNA-PK, and are processed by Artemis on the stalled replication fork *in cellulo*. This is in accord with the idea that autophosphorylation and simultaneous conformational changes in DNA-PK enhance cleavage of ssDNA–dsDNA junctions by Artemis.[6,33]

Replication-associated DSBs are thought to be one-sided DSBs, and can cause chromosomal aberrations such as translocation, when these one-sided DSBs are rejoined with incorrect partners. Indeed, replication-associated DSBs are thought to be tumorigenic.[34,35] Thus, genome integrity during replication needs to be monitored by several fail-safe mechanisms. Increase of DSB generation and apoptosis induction is one of the ways to avoid tumorigenesis in Artemis-competent cells. In contrast, induction of apoptosis was impaired and cellular survival was increased with fewer DSBs in Artemis-deficient fibroblasts after prolonged

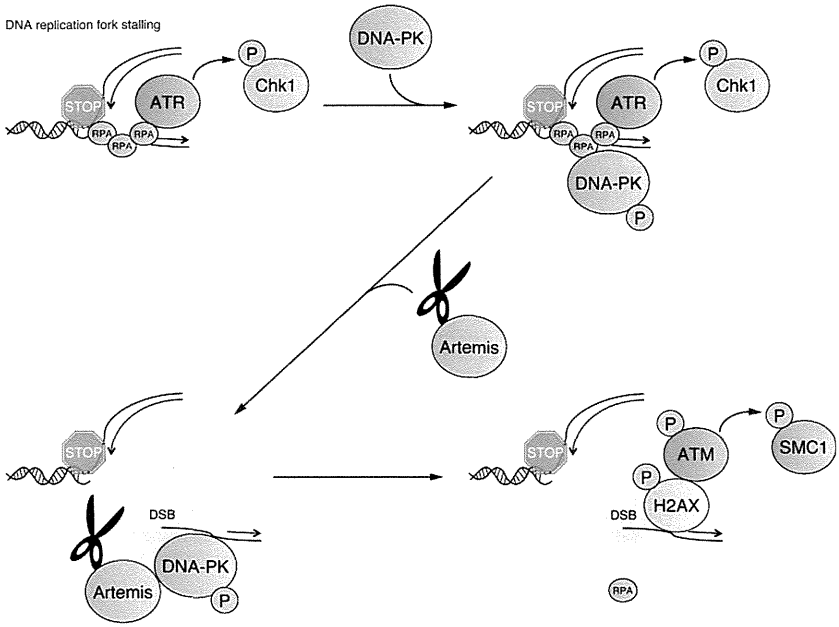

Fig. 7. Model for Artemis-mediated double-strand break (DSB) formation and subsequent DNA damage checkpoint activation. ATM, ataxia–telangiectasia mutated; ATR, ataxia–telangiectasia and RAD3-related; DNA-PK, DNA-dependent protein kinase; P, phosphorylation; RPA, replication protein A.

doi: 10.1111/cas.12144

HU.[36] Artemis-deficient fibroblasts may have aberrant chromosomes in M-phase after prolonged HU treatment, as is the case in Mus81-knockout embryonic stem cells,[19] but fail to be eradicated by cell death through apoptosis/mitotic catastrophe. These are in accord with the recent finding that apoptosis induction after massive DSB is Artemis-dependent.[37] Thus, further study is ongoing in order to assess whether genomic abnormalities increase in Artemis-deficient fibroblasts surviving after HU-induced replication stress.

In summary, our findings indicate a novel function of the DNA nuclease Artemis in resolving stalled DNA replication forks in cells in S phase, with potential implications for understanding carcinogenesis and therapeutic responses to DNA damaging drugs. Although stalled replication forks initially activate an ATR-dependent DNA damage response, when stalling is prolonged, cells may trigger a second wave of DNA damage checkpoint response mediated by Artemis-dependent DSB generation (Fig. 7). Thus, Artemis plays an essential role in the response to DNA damage caused by HU-induced replication fork stalling. Subsequent activation of the ATM signaling pathway in response to DSB generation could allow two alternative cell fates through either induction of cell death or DSB-dependent DNA repair/replication restart, thereby preventing the disruption of DNA integrity.

Acknowledgments

We thank Dr. Leonard Wu (University of Oxford, Oxford, UK) for providing the pG68 and pG48 plasmids, and Dr. Minoru Takata (Kyoto University, Kyoto, Japan) for providing the Artemis expression plasmid. We also thank N. Terada and M. Sato for characterizing Artemis-deficient fibroblasts by genomic PCR, S. Nakada, A. Shibata, R. Sakasai, and Y. Ichijima for inspiring discussions, and the members of the H.T. and S.M. laboratories for helpful discussions. This work was supported by a Grant-in-Aid from the Ministry of Education, Science, and Culture (Japan) to S.M. and by a Grant-in-Aid for Cancer Research from the Ministry of Health, Labor and Welfare (Japan) to S.M. and M.T.

Disclosure Statement

The authors have no conflicts of interest.

Abbreviations

ATM	ataxia–telangiectasia mutated
ATR	ataxia–telangiectasia and RAD3-related
DNA-PK	DNA-dependent protein kinase
DNA-PKcs	catalytic subunit of DNA-dependent protein kinase
*ds*DNA	double-stranded DNA
DSB	double-strand break
γH2AX	phosphorylated histone H2AX
hTERT	human telomerase reverse transcriptase
HU	hydroxyurea
PFGE	pulse field gel electrophoresis
RPA	replication protein A
RS-SCID	radiosensitive severe combined immunodeficiency
shRNA	short hairpin RNA
siATR	short interfering RNA against ATR
siRNA	short interfering RNA
ssDNA	single-stranded DNA

References

1 Cimprich KA, Cortez D. ATR: an essential regulator of genome integrity. *Nat Rev Mol Cell Biol* 2008; **9**: 616–27.
2 Falck J, Coates J, Jackson SP. Conserved modes of recruitment of ATM, ATR and DNA-PKcs to sites of DNA damage. *Nature* 2005; **434**: 605–11.
3 Bakkenist CJ, Kastan MB. DNA damage activates ATM through intermolecular autophosphorylation and dimer dissociation. *Nature* 2003; **421**: 499–506.
4 Jazayeri A, Falck J, Lukas C, *et al.* ATM- and cell cycle-dependent regulation of ATR in response to DNA double-strand breaks. *Nat Cell Biol* 2006; **8**: 37–45.
5 Branzei D, Foiani M. Regulation of DNA repair throughout the cell cycle. *Nat Rev Mol Cell Biol* 2008; **9**: 297–308.
6 Goodarzi AA, Yu Y, Riballo E, *et al.* DNA-PK autophosphorylation facilitates Artemis endonuclease activity. *EMBO J* 2006; **25**: 3880–9.
7 Ma Y, Schwarz K, Lieber MR. The Artemis: DNA-PKcs endonuclease cleaves DNA loops, flaps, and gaps. *DNA Repair (Amst)* 2005; **4**: 845–51.
8 Riballo E, Kuhne M, Rief N, *et al.* A pathway of double-strand break rejoining dependent upon ATM, Artemis, and proteins locating to gamma-H2AX foci. *Mol Cell* 2004; **16**: 715–24.
9 Kobayashi N, Agematsu K, Sugita K, *et al.* Novel Artemis gene mutations of radiosensitive severe combined immunodeficiency in Japanese families. *Hum Genet* 2003; **112**: 348–52.
10 Stiff T, Walker SA, Cerosaletti K, *et al.* ATR-dependent phosphorylation and activation of ATM in response to UV treatment or replication fork stalling. *EMBO J* 2006; **25**: 5775–82.
11 Sakasai R, Shinohe K, Ichijima Y, *et al.* Differential involvement of phosphatidylinositol 3-kinase-related protein kinases in hyperphosphorylation of replication protein A2 in response to replication-mediated DNA double-strand breaks. *Genes Cells* 2006; **11**: 237–46.
12 Brown EJ, Baltimore D. ATR disruption leads to chromosomal fragmentation and early embryonic lethality. *Genes Dev* 2000; **14**: 397–402.
13 Zhao H, Piwnica-Worms H. ATR-mediated checkpoint pathways regulate phosphorylation and activation of human Chk1. *Mol Cell Biol* 2001; **21**: 4129–39.
14 Liu S, Bekker-Jensen S, Mailand N, Lukas C, Bartek J, Lukas J. Claspin operates downstream of TopBP1 to direct ATR signaling towards Chk1 activation. *Mol Cell Biol* 2006; **26**: 6056–64.
15 Matsuoka S, Rotman G, Ogawa A, Shiloh Y, Tamai K, Elledge SJ. Ataxia telangiectasia-mutated phosphorylates Chk2 in vivo and in vitro. *Proc Natl Acad Sci USA* 2000; **97**: 10389–94.
16 Takahashi A, Ohnishi T. Does gammaH2AX foci formation depend on the presence of DNA double strand breaks? *Cancer Lett* 2005; **229**: 171–9.
17 Ward IM, Chen J. Histone H2AX is phosphorylated in an ATR-dependent manner in response to replicational stress. *J Biol Chem* 2001; **276**: 47759–62.
18 Robison JG, Lu L, Dixon K, Bissler JJ. DNA lesion-specific co-localization of the Mre11/Rad50/Nbs1 (MRN) complex and replication protein A (RPA) to repair foci. *J Biol Chem* 2005; **280**: 12927–34.
19 Hanada K, Budzowska M, Davies SL, *et al.* The structure-specific endonuclease Mus81 contributes to replication restart by generating double-strand DNA breaks. *Nat Struct Mol Biol* 2007; **14**: 1096–104.
20 Furuta T, Takemura H, Liao ZY, *et al.* Phosphorylation of histone H2AX and activation of Mre11, Rad50, and Nbs1 in response to replication-dependent DNA double-strand breaks induced by mammalian DNA topoisomerase I cleavage complexes. *J Biol Chem* 2003; **278**: 20303–12.
21 Shi W, Feng Z, Zhang J, *et al.* The role of RPA2 phosphorylation in homologous recombination in response to replication arrest. *Carcinogenesis* 2010; **31**: 994–1002.
22 Chan DW, Chen BP, Prithivirajsingh S, *et al.* Autophosphorylation of the DNA-dependent protein kinase catalytic subunit is required for rejoining of DNA double-strand breaks. *Genes Dev* 2002; **16**: 2333–8.
23 Chen BP, Chan DW, Kobayashi J, *et al.* Cell cycle dependence of DNA-dependent protein kinase phosphorylation in response to DNA double strand breaks. *J Biol Chem* 2005; **280**: 14709–15.
24 Hammarsten O, Chu G. DNA-dependent protein kinase: DNA binding and activation in the absence of Ku. *Proc Natl Acad Sci USA* 1998; **95**: 525–30.
25 Martensson S, Hammarsten O. DNA-dependent protein kinase catalytic subunit. Structural requirements for kinase activation by DNA ends. *J Biol Chem* 2002; **277**: 3020–9.
26 Morozov VE, Falzon M, Anderson CW, Kuff EL. DNA-dependent protein kinase is activated by nicks and larger single-stranded gaps. *J Biol Chem* 1994; **269**: 16684–8.
27 Falzon M, Fewell JW, Kuff EL. EBP-80, a transcription factor closely resembling the human autoantigen Ku, recognizes single- to double-strand transitions in DNA. *J Biol Chem* 1993; **268**: 10546–52.
28 Ralf C, Hickson ID, Wu L. The Bloom's syndrome helicase can promote the regression of a model replication fork. *J Biol Chem* 2006; **281**: 22839–46.

29 Bae JB, Mukhopadhyay SS, Liu L, *et al.* Snm1B/Apollo mediates replication fork collapse and S Phase checkpoint activation in response to DNA interstrand cross-links. *Oncogene* 2008; **27**: 5045–56.
30 Ciccia A, McDonald N, West SC. Structural and functional relationships of the XPF/MUS81 family of proteins. *Annu Rev Biochem* 2008; **77**: 259–87.
31 Burrow AA, Marullo A, Holder LR, Wang YH. Secondary structure formation and DNA instability at fragile site FRA16B. *Nucleic Acids Res* 2010; **38**: 2865–77.
32 Voineagu I, Narayanan V, Lobachev KS, Mirkin SM. Replication stalling at unstable inverted repeats: interplay between DNA hairpins and fork stabilizing proteins. *Proc Natl Acad Sci USA* 2008; **105**: 9936–41.
33 Ding Q, Reddy YV, Wang W, *et al.* Autophosphorylation of the catalytic subunit of the DNA-dependent protein kinase is required for efficient end processing during DNA double-strand break repair. *Mol Cell Biol* 2003; **23**: 5836–48.
34 Bartkova J, Horejsi Z, Koed K, *et al.* DNA damage response as a candidate anti-cancer barrier in early human tumorigenesis. *Nature* 2005; **434**: 864–70.
35 Gorgoulis VG, Vassiliou LV, Karakaidos P, *et al.* Activation of the DNA damage checkpoint and genomic instability in human precancerous lesions. *Nature* 2005; **434**: 907–13.
36 Unno J. Artemis-dependent cell death by prolonged replication fork stalling. *Jpn J Pediatr Hematol.* 2011; **25**: 86–90.
37 Abe T, Ishiai M, Hosono Y, *et al.* KU70/80, DNA-PKcs, and Artemis are essential for the rapid induction of apoptosis after massive DSB formation. *Cell Signal* 2008; **20**: 1978–85.

Supporting Information

Additional Supporting Information may be found in the online version of this article:

Doc. S1. Supplementary experimental procedure.

Fig. S1. Cell cycle distribution of S-phase synchronized HeLa cells, quantification of Figure 1(b); ATM activation in HeLa cells transfected with siATR, quantification of Fig. 1(b) .

Fig. S2. Magnified image of γH2AX and RPA2 foci and signal intensity chromatographs.

Fig. S3. RPA2 and phosphorylated ATM colocalization after hydroxyurea treatment, analyzed by immunofluorescence.

Fig. S4. Camptothecin (CPT) induces double-strand breaks.

Fig. S5. Cell cycle profiles of shRNA transfected HeLa cells.

Fig. S6. Quantitation of immunofluorescence data shown in Figure 5(b). Magnified image of phospho-DNA-PKcs (T2609) and RPA2 fociand signal intensity chromatographs. Artemis-independent activation of DNA-PKcs analyzed by Western blotting and immunofluorescence.

Fig. S7. Generation of DSBs dependent on DNA-PKcs analyzed by comet assay.

doi: 10.1111/cas.12144

免疫細胞療法
細胞培養ガイドライン

平成 25 年 11 月 12 日制定

日本免疫学会

日本がん免疫学会

日本バイオセラピィ学会

癌免疫外科研究会

血液疾患免疫療法研究会

日本免疫治療学研究会

目次